MOLECULAR AND CELLULAR BIOLOGY, Sept. 2004, p. 7758–7768 Vol. 24, No. 17
0270-7306/04/$08.00+0 DOI: 10.1128/MCB.24.17.7758–7768.2004

Mice with Deficiency of G Protein γ_3 Are Lean and Have Seizures

William F. Schwindinger,[1] Kathryn E. Giger,[1] Kelly S. Betz,[1] Anna M. Stauffer,[1] Elaine M. Sunderlin,[1] Laura J. Sim-Selley,[2] Dana E. Selley,[2] Sarah K. Bronson,[3] and Janet D. Robishaw[1]*

Weis Center for Research, Geisinger Clinic, Danville,[1] and Department of Cellular and Molecular Physiology, The Pennsylvania State College of Medicine, Hershey,[3] Pennsylvania, and Department of Pharmacology and Toxicology, Virginia Commonwealth University, Richmond, Virginia[2]

Received 26 February 2004/Returned for modification 3 April 2004/Accepted 13 June 2004

Emerging evidence suggests that the γ subunit composition of an individual G protein contributes to the specificity of the hundreds of known receptor signaling pathways. Among the twelve γ subtypes, γ_3 is abundantly and widely expressed in the brain. To identify specific functions and associations for γ_3, a gene-targeting approach was used to produce mice lacking the *Gng3* gene (*Gng3*$^{-/-}$). Confirming the efficacy and specificity of gene targeting, *Gng3*$^{-/-}$ mice show no detectable expression of the *Gng3* gene, but expression of the divergently transcribed *Bscl2* gene is not affected. Suggesting unique roles for γ_3 in the brain, *Gng3*$^{-/-}$ mice display increased susceptibility to seizures, reduced body weights, and decreased adiposity compared to their wild-type littermates. Predicting possible associations for γ_3, these phenotypic changes are associated with significant reductions in β_2 and α_{i3} subunit levels in certain regions of the brain. The finding that the *Gng3*$^{-/-}$ mice and the previously reported *Gng7*$^{-/-}$ mice display distinct phenotypes and different αβγ subunit associations supports the notion that even closely related γ subtypes, such as γ_3 and γ_7, perform unique functions in the context of the organism.

The G protein βγ dimer performs numerous roles in the signal transduction process, from membrane targeting of the α subunit (12), to recognition of receptors (23), to activation of effectors (7), to modulation of various proteins affecting the signal intensity or duration (24). In fact, there is potential for a large number of different βγ dimers arising from combinatorial association of the 5 β and 12 γ subtypes. The current challenge is to identify which of these βγ dimers actually exist in vivo and to establish their roles in particular signaling pathways and biological processes. Although transfection and reconstitution provide valuable information on the potential interactions of the β and γ subtypes, these strategies fall short of identifying their actual associations and functions in the context of the organism. By contrast, a gene deletion approach represents a powerful method for determining this information by analyzing the resulting phenotype in knockout mice.

The γ_3 subtype has characteristic features that led us to believe that mice with a targeted disruption of *Gng3* would display a distinctive phenotype. *Gng3* is predominantly expressed in the brain (1, 5, 17), where its expression increases during postnatal development (1, 34). Within the brain, γ_3 is widely expressed in neurons rather than glial cells (2, 22, 33). In vitro RNA suppression studies predict a specific function for γ_3 in coupling various receptors to changes in calcium channel activity (9, 25, 26). These in vitro studies also suggested that γ_3 functions in several different heterotrimer combinations: $\alpha_{o2}\beta_1\gamma_3$ (9), $\alpha_{13}\beta_1\gamma_3$ (26), and $\alpha_{q/11}\beta_{1/3}\gamma_3$ (25).

In the present study, we show that *Gng3*$^{-/-}$ mice exhibit changes in seizure susceptibility and body weight on both mixed and C57BL/6J genetic backgrounds. Although the receptor signaling pathway(s) responsible for this complex phenotype is not yet identified, we show that loss of the γ_3 subunit produces concurrent reductions in levels of the β_2, β_1, and α_{i3} subunits in certain brain regions and that a deficiency of the γ_3 subunit does not impair regulation of adenylyl cyclase activity. In a previous study, Schwindinger et al. generated mice lacking the *Gng7* gene, which encodes the γ_7 subtype, and identified a unique function for γ_7 together with α_{olf} in stimulation of adenylyl cyclase activity in the striatum (39). Comparison of *Gng3*$^{-/-}$ mice and *Gng7*$^{-/-}$ mice reveals different phenotypes, different heterotrimeric partners, and different signal transduction pathways, demonstrating the unique functions of these two G protein γ subtypes in vivo.

MATERIALS AND METHODS

Production of mice. Targeted embryonic stem cells, chimeric mice, and F_1 heterozygotes with a floxed *Gng3* allele (*Gng3*$^{+/fl}$) were produced at Lexicon Genetics, Inc. (The Woodlands, Tex.). To provide the potential for conditional inactivation of *Gng3* in future studies, the targeting vector included a 1.9-kb cassette containing a *loxP* site and a PGK-*neo*^{R} selectable marker in the first intron (52 bp upstream of the initiation codon), and a second, 59-bp *loxP* cassette in the 3′ untranslated region (immediately downstream of the termination codon). *Gng3*$^{+/fl}$ mice were bred to mice carrying the *Cre* recombinase driven by the EIIa adenovirus promoter, FVB/N-Tgn(EIIa-Cre)C5379Lmgd (Jackson Laboratory, Bar Harbor, Maine), to produce mice bearing the deleted *Gng3* allele (*Gng3*$^-$). *Gng3*$^{+/-}$ mice were then backcrossed to C57BL/6J mice (Jackson Laboratory) for 5 generations. *Gng3*$^{+/-}$ mice were intercrossed to produce the mice used in these studies, either before (i.e., N_0 backcross) or after (i.e., N_5 backcross) 5 backcrosses to C57BL/6J mice.

Animal care and approval. Mice were segregated by sex and group housed in ventilated racks (Thoren Caging Systems, Inc., Hazelton, Pa.). Mice were given access to water and Mouse Diet 9F (Purina Mills, LLC, St. Louis, Mo.) ad libitum. Environmental factors included temperature and humidity control and a 12-h light-dark cycle. Mice were maintained as virus antibody free and parasite free. Animal research protocols were approved by the Geisinger Clinic institutional animal care and use committee.

* Corresponding author. Mailing address: Geisinger Clinic, Weis Center for Research, 100 North Academy Ave., Danville, PA 17822. Phone: (570) 271-6684. Fax: (570) 271-6701. E-mail: jrobishaw@geisinger.edu.

TABLE 1. Primers used in this study

Name	Description[a]	Sequence
JR282	*Gng3* 3′ UTR antisense	GAG TAG AAG GTG CTT GGA GT
JR289	*Gng3* exon 1 sense	ACG CAA GAT GGT GGA ACA GC
JR416	*Gng3* 5′ sense	TCT GGG CAG AAC TTA AGC TG
JR353	*Cre* sense	GTT CGC AAG AAC CTG ATG GAC A
JR354	*Cre* antisense	CTA GAG CCT GTT TTG CAC GTT C
JR175	*Eef1a2* sense	GGA ATG GTG ACA ACA TGC TG
JR174	*Eef1a2* antisense	CGT TGA AGC CTA CAT TGT CC
JR443 (a)	*Bscl2* antisense	TAG TGG AAG TGC ACA GGG CTG
JR444	*Bscl2* common sense	GAC CCA CCG TTC TTC AGA GCT
JR445 (b)	*Bscl2* exon 1 sense	CCT GAC ACA GCA CTT AGC ACC
JR446 (c)	*Bscl2* alt exon 1 sense	ACG TTG TCC TCT GAG GCT CTG
Gapds	*Gapd* sense	TGA AGG TCG GTG TGA ACG GAT TTG GC
Gapdas	*Gapd* antisense	CAT GTA GGC CAT GAG GTC ACC AC

[a] UTR, untranslated region; alt, alternate.

Genotyping. Southern blot analysis was performed on genomic tail DNA digested with HindIII. The probe used for this analysis was a 1-kb fragment 3′ of the modified *Gng3* allele. Alternatively, PCR analysis was performed using primers (Invitrogen, Rockville, Md.) shown in Table 1. Briefly, primers flanking the 3′ *loxP* site (JR282 and JR286) were used to competitively amplify the *Gng3* and *Gng3*^{fl} alleles, while a third primer, upstream of the 5′ *loxP* site (JR416), was included to simultaneously amplify the *Gng3*$^{-}$ allele. The bacteriophage P1 *Cre* transgene was amplified with JR353 and JR354.

Expression of the *Gng3* and *Bscl2* genes. PCR amplification of cDNA in the murine multiple tissue cDNA panel (BD Biosciences, Palo Alto, Calif.) was performed according to the manufacturer's instructions. RNA was isolated from whole brain or adipose tissues by using TRIzol reagent (Invitrogen). First-strand cDNA was prepared from 2 μg of RNA by using Moloney murine leukemia virus reverse transcriptase (Promega), and this was used as a template to amplify the *Gng3*, *Bscl2*, or elongation factor transcripts with the primers shown in Table 1.

Audiogenic seizures. Audiogenic seizures were induced in 6- to 12-week-old mice (21). Mice were placed in a clear plastic breeding box (27 by 27 by 20 cm) with a filter paper lid and were allowed to explore for 1 min. Five metal keys on a ring were shaken above the box for 10 s to produce a sound of 85 to 95 dB near the bottom of the box, as measured with a sound level meter (Tandy Corp., Fort Worth, Tex.). Observation was continued for at least 1 min after cessation of the sound. All sessions were videotaped and then graded by two observers who were unaware of the genotypes of the mice.

Immunoblot analysis. To examine the expression of G protein subunits in the brain, Western blot analysis was performed on cholate-solubilized membranes prepared from the cortex, hippocampus, cerebellum, striatum, or whole brain, as described previously (39). Antisera for Ras (BD Biosciences) and for the rat Na^+/K^+-ATPase β subunit (Research Diagnostics, Inc., Flanders, N.J.) were used at a 1:2,000 dilution. Antisera for α_{i1}, α_{i3}, and $\alpha_{q/11}$ (Calbiochem, La Jolla, Calif.) were used at a 1:1,000 dilution. Antisera for $\alpha_{i1/i3}$, α_{i2}, α_o (1:500), β_1 (1:500), β_2 (1:500), γ_2, γ_3, γ_5 (1:100), and γ_7 have been described previously (5, 13, 47) and were used at a 1:200 dilution except as indicated. Antisera for α_s (a generous gift from Catherine Berlot) were used at a 1:500 dilution, antisera for α_{olf} (a generous gift from Denis Hervé) were used at 1:2,000, and antisera for α_{12} or α_{13} (generous gifts from N. Dhanasekaran) were used at 1:1,000. His-tagged G protein subunits (CytoSignal Research Products, Irvine, Calif.) were used as standards for quantitative immunoblotting.

GTPγS binding assay. Agonist-stimulated [^{35}S]GTPγS autoradiography was performed as previously described (32, 43) with slight modifications. Following CO_2 euthanasia, brains were removed and frozen in isopentane at −35°C. Coronal sections (thickness, 20 μm) at the levels of the striatum and hippocampus were cut on a cryostat at −20°C and mounted on gelatin-coated slides. Slides were equilibrated in 50 mM Tris-HCl–3 mM $MgCl_2$–0.2 mM EGTA–100 mM NaCl (pH 7.4) (assay buffer) at 25°C for 10 min and were then preincubated in assay buffer containing 2 mM GDP and adenosine deaminase (9.5 mU/ml) at 25°C for 15 min. Assays were conducted by incubating slides in assay buffer with 2 mM GDP, adenosine deaminase (9.5 mU/ml), and 0.04 nM [^{35}S]GTPγS (250 Ci/mmol; New England Nuclear Corp., Boston, Mass.) with (stimulated) or without (basal) agonist at 25°C for 2 h. Agonists included [D-Ala^2,N-Me-Phe^4,Gly^5-ol]-enkephalin (DAMGO) (Drug Supply Program, National Institute on Drug Abuse), WIN 55,212-2, and (−)-N^6-(2-phenylisopropyl)adenosine (PIA) (Sigma Chemical Co., St. Louis, Mo.) at a concentration (10 μM) that has been shown to produce maximal, antagonist-reversible stimulation (32, 43). Slides were rinsed twice in 50 mM Tris-HCl, pH 7.4, at 4°C for 2 min each time and then in H_2O at 4°C for 30 s. Slides were dried overnight and exposed to Biomax MR film (Eastman Kodak Co., Rochester, N.Y.) for 24 h in the presence of ^{14}C-labeled microscales. Films were digitized with a Sony XC-77 video camera and analyzed by using the NIH IMAGE program for Macintosh computers. Net agonist-stimulated [^{35}S]GTPγS binding was calculated by subtracting basal binding from agonist-stimulated binding. Data are reported as means ± standard errors for triplicate sections of brains from six mice per group. Statistical comparison between wild-type and knockout mice was performed by analysis of variance followed by post hoc analysis using the two-tailed nonpaired Student *t* test.

Adenylyl cyclase assay. Membranes were prepared as previously described (39) from cerebellums of *Gng3*$^{-/-}$ and *Gng3*$^{+/+}$ mice. Adenylyl cyclase activity was determined by incubating membranes (20 μg of protein) at 30°C for 10 min in a solution containing 0.1 ml of an agonist-specific buffer, 0.5 μCi of [α-^{32}P]ATP, 0.1 mM ATP, 0.05 mM GTP, and an ATP regenerating system consisting of 5 mM creatine phosphate and 50 U of creatine phosphokinase/ml. For the A_1 adenosine agonist, cyclopentyl adenosine (10 to 1,000 nM), the buffer consisted of 50 mM HEPES (pH 7.4), 1 mM EGTA, 5 mM $MgCl_2$, 0.01 mM rolipram, and 1 U of adenosine deaminase/ml (30). For the cannabinoid agonist anandamide (1 to 10 μM), the buffer consisted of 50 mM Tris · HCl (pH 7.4), 2 mM $MgSO_4$, 0.5 mM 3-isobutyl-1-methylxanthine (IBMX), and 0.03 mM cAMP (6). Reactions were terminated by addition of 0.1 ml of 2% sodium dodecyl sulfate, 40 mM ATP, 1.4 mM cAMP, and 0.06 μCi of [2,8-^{3}H]cAMP and heating to 95°C for 3 min. The resulting [^{32}P]cAMP and the added [^{3}H]cAMP were isolated by Dowex and alumina chromatography (19) and quantified in an LS-6500 scintillation counter (Beckman) using ScinitiSafe Plus 50% LSC-Cocktail (Fisher).

RESULTS

Targeted disruption of the *Gng3* gene. Mice with a targeted deletion of the *Gng3* gene were produced in two steps (Fig. 1A). First, mice with a floxed *Gng3* allele (*Gng3*^{fl}) were created by using a targeting vector in which the complete coding region of the gene was flanked by *loxP* sites. This provides the potential for generation of inducible or tissue-specific knockouts in future studies. Second, mice with a deleted *Gng3* allele (*Gng3*$^{-}$) were produced by crossing *Gng3*^{fl} mice with mice expressing the *Cre* transgene under the control of the EIIa adenovirus promoter. As shown by Southern blot analysis, this resulted in the excision of the complete coding region of the *Gng3* gene (Fig. 1B). To produce the mice used in subsequent experiments, mice carrying the *Gng3*$^{-}$ allele were either intercrossed, to obtain mice on a mixed genetic background, or backcrossed for 5 generations, to produce mice on a C57BL/6J genetic background. PCR analysis was used to identify mice carrying the *Gng3*$^{-}$ allele (Fig. 1C). Heterozygous crosses produced litters of the expected size (6.2 ± 3.3 pups) in the

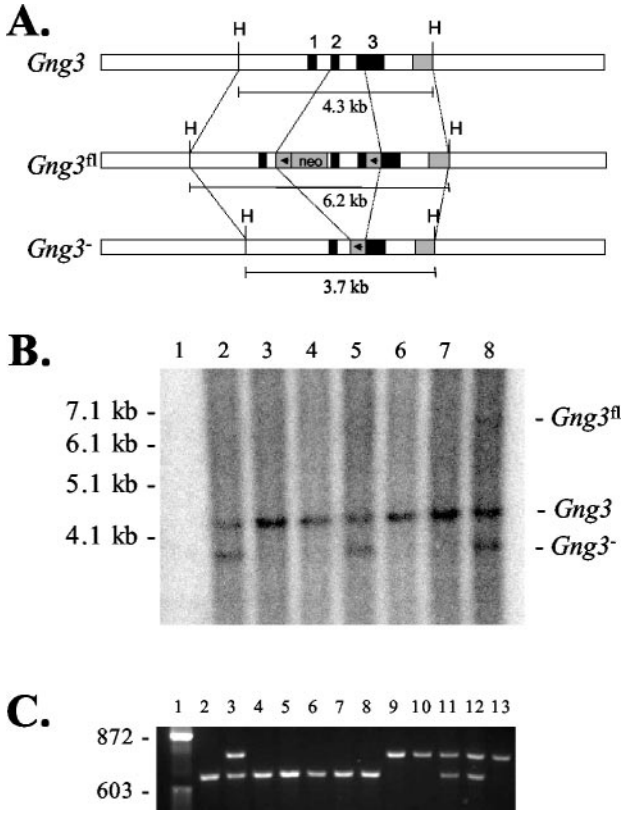

FIG. 1. (A) Targeting strategy. (Top) Wild-type allele (*Gng3*) with exons 1 to 3 (solid boxes) and the 3′ probe (shaded box). (Center) Targeted allele (*Gng3*^{fl}) with a *loxP-neo*^{R} cassette in intron 1 (arrowhead and "neo") and a *loxP* cassette in the 3′ untranslated sequence (arrowhead). (Bottom) Deleted allele (*Gng3*$^{-}$) with one remaining *loxP* site (arrowhead) following *Cre*-mediated excision of the coding region of *Gng3*. Expected sizes of HindIII (H) fragments are indicated. (B) Southern blot of tail biopsy DNA digested with HindIII and detected with the 3′ probe. Lane 1, molecular weight ladder; lanes 2 to 8, progeny of a *Gng3*$^{+/fl}$ × TgN(EIIa-Cre) cross, with all lanes showing the 4.3-kb wild-type *Gng3* allele and lanes 2, 5, and 8 also showing the 3.7-kb *Gng3*$^{-}$ allele. A small amount of residual *Gng3*^{fl} allele can be seen in lane 8. (C) PCR products obtained with primers JR282, JR286, and JR416 of tail biopsy DNA from progeny of a *Gng3*$^{+/-}$ × *Gng3*$^{+/-}$ cross. Lane 1, ϕX HaeIII marker; lanes 2 and 4 to 8, wild-type mice with a single 629-bp band derived from primers JR282 and JR286; lanes 9, 10, and 13, *Gng3*$^{-/-}$ mice with a single 755-bp band derived from primers JR282 and JR416; lanes 3, 11, and 12, heterozygous *Gng3*$^{+/-}$ mice with both bands.

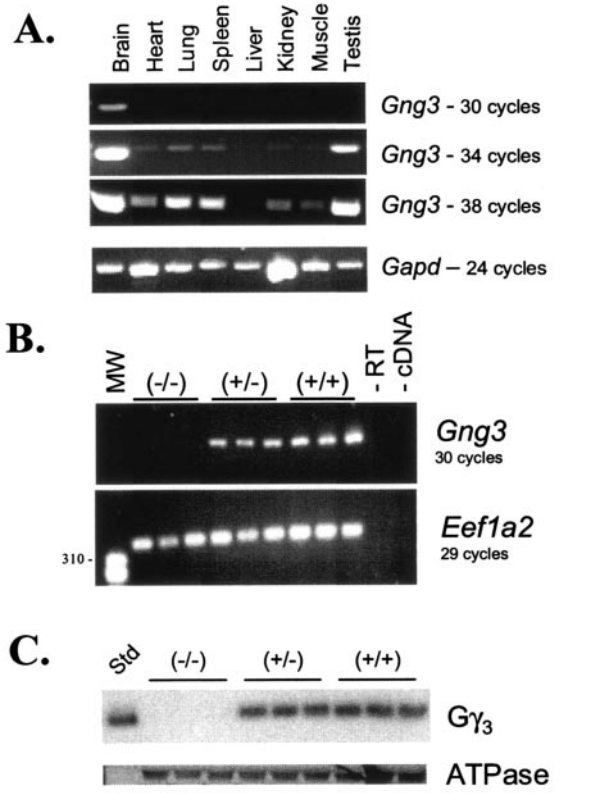

FIG. 2. (A) RT-PCR products obtained after 30, 34, or 38 cycles of amplification with primers JR282 and JR286, showing relative expression of *Gng3* in various tissues (top three panels), or products from 24 cycles with primers for glyceraldehyde-3-phosphate dehydrogenase (*Gapd*), confirming approximately equal amounts of cDNA in all reactions (bottom panel). (B) (Top) RT-PCR products obtained after 30 cycles of amplification with primers JR282 and JR286 for *Gng3*, from cDNA prepared from whole brains of three wild-type, three *Gng3*$^{+/-}$, and three *Gng3*$^{-/-}$ mice, without added reverse transcriptase (−RT), or without added cDNA (−cDNA). (Bottom) RT-PCR products obtained after 29 cycles of amplification with primers JR174 and JR175 for elongation factor 1 α2 (*Eef1a2*), from identical aliquots of the cDNAs. (C) Western blot analysis of proteins prepared from Sf9 cells expressing γ_3 (Std) or brains of three *Gng3*$^{-/-}$, three *Gng3*$^{+/-}$, and three wild-type mice. Top panel shows that γ_3 is reduced in membranes from *Gng3*$^{+/-}$ mice and absent in membranes from *Gng3*$^{-/-}$ mice. Bottom panel shows that sodium/potassium ATPase β-subunit levels are equal in all lanes.

expected 1:2:1 ratio (112 *Gng3*$^{+/+}$ pups, 225 *Gng3*$^{+/-}$ pups, and 119 *Gng3*$^{-/-}$ pups), indicating that disruption of *Gng3* does not affect survival to weaning. In sequential matings of one homozygous pair, *Gng3*$^{-/-}$ mice were fertile and weaned litters of apparently normal size (9.3 ± 1.2 pups).

Abolished expression of the *Gng3* gene. To confirm the effectiveness of the targeted gene deletion, expression of *Gng3* was examined in the brain, where the gene was most highly expressed (Fig. 2A). Reverse transcription-PCR (RT-PCR) analysis demonstrated that γ_3 mRNA was present at reduced levels in brains from *Gng3*$^{+/-}$ mice and was absent in brains from *Gng3*$^{-/-}$ mice (Fig. 2B). Likewise, Western blot analysis with γ_3-specific antisera (20) showed that the γ_3 protein was reduced by 35% ± 5% in cholate-solubilized membrane extracts of brains from *Gng3*$^{+/-}$ mice and was not detected in brains from *Gng3*$^{-/-}$ mice (Fig. 2C).

Preserved expression of the *Bscl2* gene. The *Gng3* gene is located head-to-head with the *Bscl2* gene, previously known as *Gng3lg* (10). Because of this arrangement, these two genes may share promoter elements. Moreover, our analysis of expressed sequence tags (e.g., GenBank accession no. CB566482 and BI855301) reveals the existence of an alternate first exon that places the *Gng3* gene within the alternate first intron of the *Bscl2* gene (Fig. 3A). To rule out the possibility that mice carrying the *Gng3*$^{-}$ allele may show altered expression of the *Bscl2* gene, RT-PCR analysis was performed on total RNA obtained from brains and adipose tissue. This analysis showed that both *Bscl2* mRNA transcripts were expressed at comparable levels in brains from *Gng3*$^{+/+}$, *Gng3*$^{+/-}$, and *Gng3*$^{-/-}$

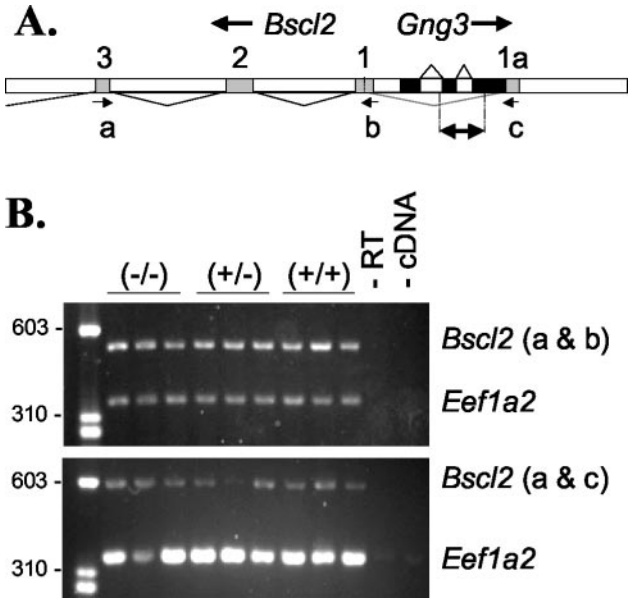

FIG. 3. (A) Organization of the *Bscl2* and *Gng3* genes, showing the first few exons (exons 1 to 3) of *Bscl2* (shaded boxes), including the alternate exon 1 (1a), and the three exons of *Gng3* (solid boxes). The region replaced in the targeted allele, $Gng3^{-}$, is indicated by the double arrow. Arrows mark positions of primers used for amplification of *Bscl2*: the antisense primer JR443 (a), the exon 1-specific sense primer JR445 (b), and the alternate exon 1-specific sense primer JR446 (c). (B) Duplex RT-PCR of brain cDNA from three $Gng3^{-/-}$ (−/−), three $Gng3^{+/-}$ (+/−), and three wild-type (+/+) mice, with primers for exon 1 of *Bscl2* (upper panel), the alternate exon 1 of *Bscl2* (lower panel), and elongation factor *Eef1a2* (both panels), showing approximately equal levels of either *Bscl2* transcript across all genotypes.

mice (Fig. 3B). Likewise, *Bscl2* mRNA transcripts were detected at similar levels in white or brown adipose tissue from $Gng3^{+/+}$ and $Gng3^{-/-}$ mice (data not shown). Taken together, these results show that *Gng3* deletion produces loss of γ_3 mRNA and protein (Fig. 2) without affecting the expression of the closely linked *Bscl2* gene.

Increased seizure susceptibility of $Gng3^{-/-}$ mice. $Gng3^{-/-}$ mice exhibit increased susceptibility to seizures, consistent with the normally high expression of *Gng3* in the brain. This was first observed on a mixed genetic background (i.e., N_0 backcross) when animal workers noticed that $Gng3^{-/-}$ mice suffered from recurrent seizures upon cage changing. Overall, 24% of $Gng3^{-/-}$ mice were observed to have recurrent handling-induced seizures, with the earliest seizure occurring at the age of 2 months. In comparison, 8% of wild-type littermates were observed to have seizures, with the earliest occurring at 14 months. These seizures were characterized by vocalizations, excessive salivation, wild running, explosive jumping, tonic-clonic convulsions, and tonic hindlimb extension. Moreover, the occurrence of these seizures was associated with a reduced life span. Approximately 40% of the $Gng3^{-/-}$ mice died between the ages of 2 months and 1 year compared to 10% of wild-type littermates over the same observation period. Because they showed no prior clinical signs, we suspect that the $Gng3^{-/-}$ mice on a mixed genetic background were dying as a result of their recurrent seizures.

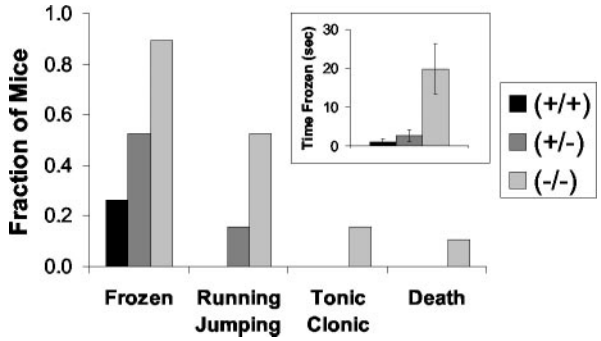

FIG. 4. Audiogenic seizures induced by a 90-dB noise with a duration of 10 s for mice on a C57BL/6J genetic background (i.e., N_5 backcross). The fraction of mice displaying a seizure of the indicated severity is shown by genotype for $Gng3^{-/-}$, $Gng3^{+/-}$, and wild-type mice (19 mice in each group). Note that $Gng3^{-/-}$ mice were more likely to demonstrate any seizure-like activity and more often progressed to more severe seizures. (Inset) Time frozen in response to auditory stimulus by genotype. Note that $Gng3^{-/-}$ mice remained frozen for significantly longer than their wild-type littermates.

Intriguingly, none of the $Gng3^{-/-}$ mice on the C57BL/6J background (i.e., N_5 backcross) were observed to have seizures upon cage changing. Moreover, the absence of these seizures was associated with an increased life span. Nevertheless, the $Gng3^{-/-}$ mice on the C57BL/6J background still showed an increased frequency and severity of seizures induced by other means (Fig. 4). In response to a loud noise, 90% of $Gng3^{-/-}$ mice exhibited mild seizure activity that was characterized by freezing for a mean time of 19.8 ± 6.5 s. In addition, 50% of $Gng3^{-/-}$ mice displayed moderate seizure activity that was characterized by wild running and explosive jumping; 15% of $Gng3^{-/-}$ mice displayed severe seizure activity that was characterized by tonic-clonic convulsions with extension; and 10% of $Gng3^{-/-}$ mice died. In contrast, only 25% of their wild-type littermates displayed even the mildest form of seizure activity that was characterized by freezing for a mean time of 1.8 ± 0.8 s. $Gng3^{+/-}$ mice had an intermediate frequency and severity of audiogenic seizures. Taken together, these results indicate that $Gng3^{-/-}$ mice on different genetic backgrounds show increased susceptibility to seizures induced by various means, suggesting a role for γ_3 in the regulation of neuronal excitability.

Reduced weight and decreased adiposity of $Gng3^{-/-}$ mice. $Gng3^{-/-}$ mice also displayed reduced body weights. This was first observed on a mixed genetic background and was later confirmed on a C57BL/6J background (Fig. 5A and B). Although indistinguishable at weaning, the $Gng3^{-/-}$ mice on the C57BL/6J background failed to gain weight at the same rate as wild-type littermates. This difference was most pronounced among female $Gng3^{-/-}$ mice, which weighed approximately 25% less than their wild-type siblings by the age of 1 year. Female $Gng3^{-/-}$ mice also showed a striking reduction in inguinal and retroperitoneal fat pad masses (Fig. 5C). This effect was associated with a dramatic decrease in serum leptin levels among female $Gng3^{-/-}$ mice (Fig. 5D). Consistent with the smaller difference in body weight, male $Gng3^{-/-}$ mice showed no significant reduction in fat pad masses (Fig. 5B and C). Taken together, these results indicate that $Gng3^{-/-}$ mice

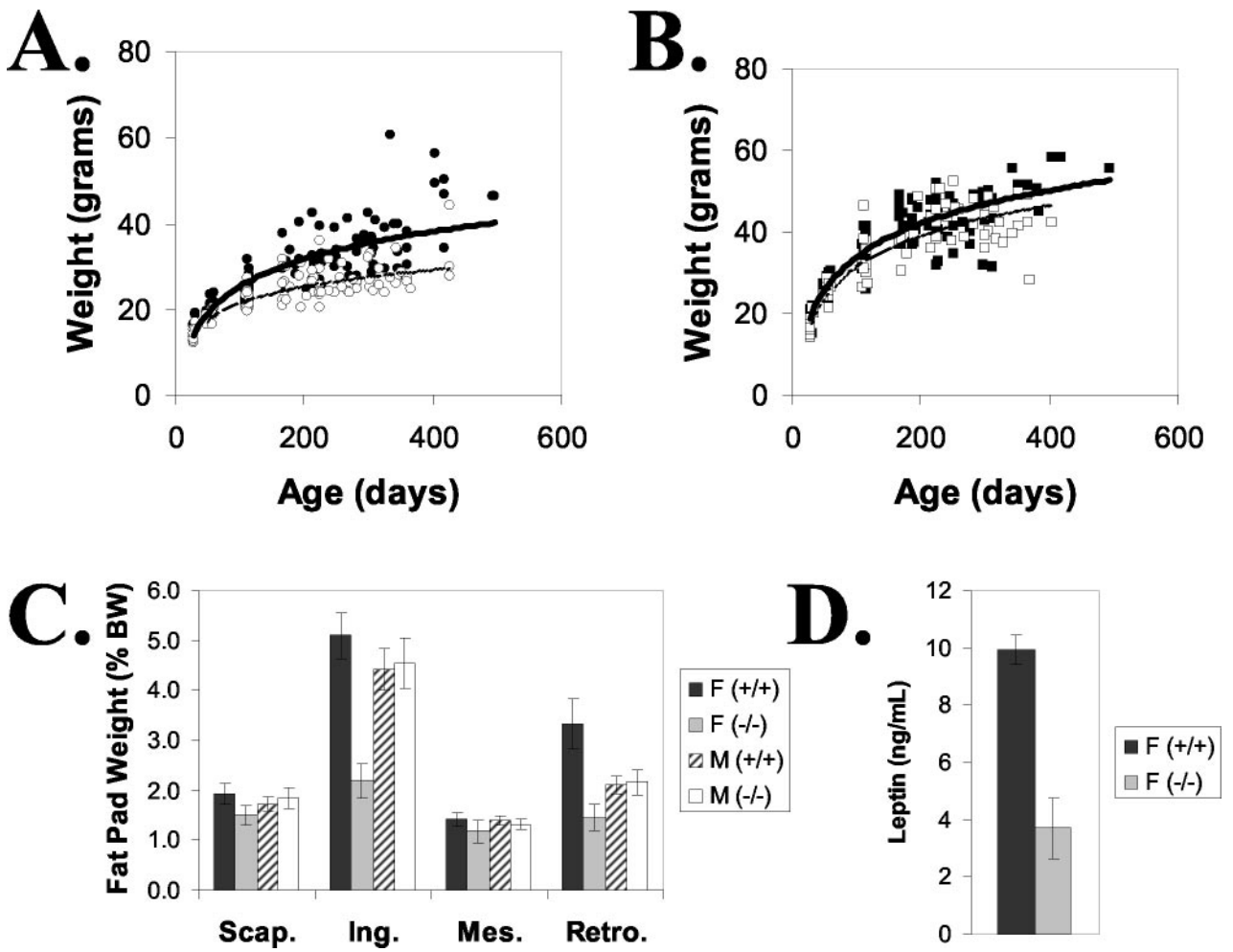

FIG. 5. Lean phenotype of *Gng3*$^{-/-}$ mice on C57BL/6J genetic background (i.e., N_5 backcross). (A) Older, female *Gng3*$^{-/-}$ mice (open circles) weighed less than wild-type littermates (filled circles). (B) Weight differences for male *Gng3*$^{-/-}$ mice (open squares) and wild-type littermates (filled squares) were not as pronounced. Weights were obtained at 3 to 9 irregular intervals, between the ages of 4 and 70 weeks, for 14 to 18 mice in each group. (C) Fat pad weights expressed as a percentage of body weight (% BW). Female *Gng3*$^{-/-}$ mice had significantly reduced inguinal (Ing.) and retroperitoneal (Retro.) fat pad weights, but interscapular (Scap.) and mesenteric (Mes.) fat pad weights were unchanged. Fat pad weights of male *Gng3*$^{-/-}$ mice were not different from those of wild-type littermates. Data are means ± standard errors for five to seven mice in each group. (D) Serum leptin levels were significantly reduced in female *Gng3*$^{-/-}$ mice. Data are means ± standard errors for five or six mice in each group.

on different genetic backgrounds exhibit reduced body weights, suggesting an additional role for γ_3 in the regulation of appetite and/or metabolism.

Possible basis for altered phenotype of *Gng3*$^{-/-}$ mice. The existence and disparate nature of the phenotypes in *Gng3*$^{-/-}$ mice indicate a requirement for γ_3 in different brain regions or distinct signaling pathways affecting neuronal excitability and body weight regulation that cannot be compensated for by related subtypes. Of the known γ subtypes, γ_2, γ_3, and γ_7 are highly expressed in the brain, where they show partly overlapping patterns of expression in the cortex, striatum, hippocampus, and cerebellum (2). To determine whether loss of γ_3 produces compensatory changes in the expression of other γ subtypes, we performed immunoblot analysis to compare the levels of various γ subtypes in several brain regions from *Gng3*$^{+/+}$ and *Gng3*$^{-/-}$ mice (Fig. 6A). The nature and extent of the observed changes were found to differ between brain regions (Fig. 6B). In this regard, γ_2 levels were increased slightly, by 23% ± 10%, in the cortices of *Gng3*$^{-/-}$ mice, while γ_7 levels were increased modestly, by 31% ± 10%, in the striatum, and the level of γ_5 was not altered in any of the brain regions examined from these animals. To provide a physiological context for the observed changes, we next performed quantitative immunoblot analysis to determine the concentrations of γ_2, γ_3, and γ_7 in these regions (Fig. 6C). In wild-type mice, γ_3 and γ_7 are expressed at comparable levels in the striatum, while γ_2 and γ_3 are detected at roughly similar levels in the cortex. Thus, the relatively small increases in γ_7 subunit levels in the striatum and γ_2 subunit levels in the cortex would not be expected to fully compensate for the loss of γ_3 subunit in *Gng3*$^{-/-}$ mice.

Possible G protein subunit associations revealed by *Gng3*$^{-/-}$ mice. Under physiological conditions, G proteins function as heterotrimers whose specific αβγ subunit combi-

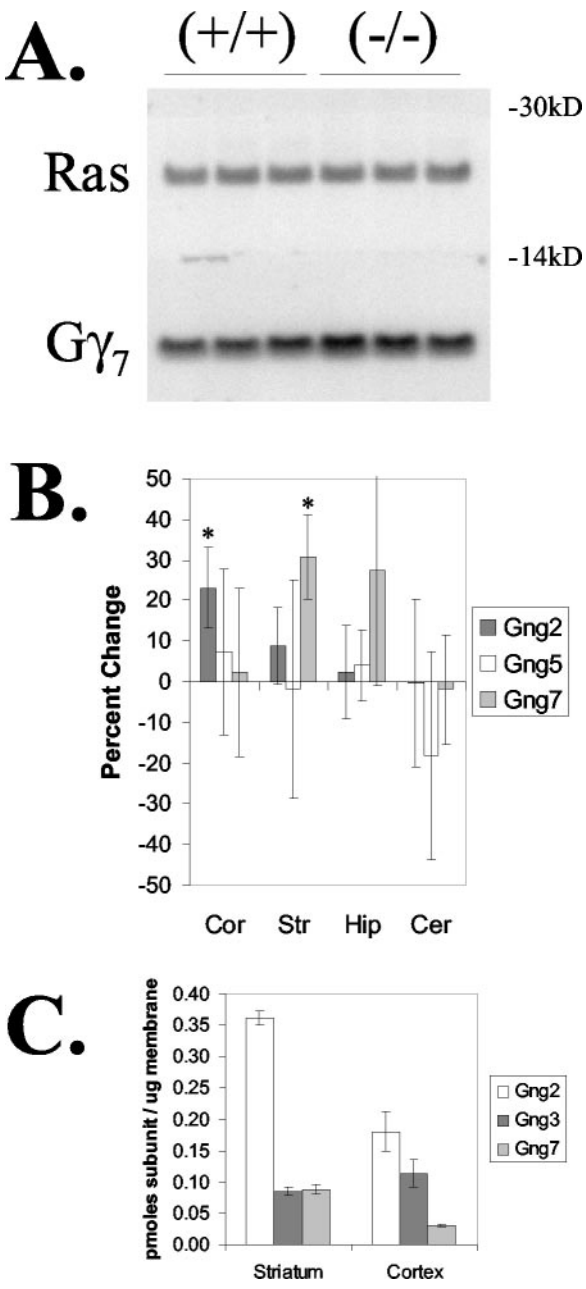

FIG. 6. Expression of other γ subtypes. (A) Representative immunoblot of cholate-extractable membrane protein (20 μg) from striata of three wild-type (+/+) and three *Gng3*$^{-/-}$ (−/−) mice. The top portion of the blot was incubated with a Ras antiserum to correct for variations in protein loading. The bottom portion was incubated with a γ_7 antiserum. Note the increased level of γ_7 in the striata of *Gng3*$^{-/-}$ mice. (B) Quantification of immunoblots for γ_2 (Gng2), γ_5 (Gng5), and γ_7 (Gng7) in the cortex (Cor), striatum (Str), hippocampus (Hip), and cerebellum (Cer). Relative levels in *Gng3*$^{-/-}$ mice are shown as the percent change from levels in wild-type mice. Data are means ± standard deviations for three mice in each group. *, $P < 0.05$ for comparison of *Gng3*$^{-/-}$ to *Gng*$^{+/+}$ mice by Student's *t* test. (C) Concentrations of γ_2, γ_3, and γ_7 in the cortex and striatum, showing approximately equimolar amounts of γ_2 and γ_3 in the cortex and of γ_3 and γ_7 in the striatum. Data are expressed as picomoles of γ subunit per microgram of membrane cholate extract and are means ± standard errors for three or four wild-type mice.

nations determine their particular roles in receptor signaling pathways (37). Increasing evidence suggests that the composition of the γ subunit may play a critical role in the assembly of specific αβγ subunit combinations. In this regard, it was shown previously that loss of γ_7 coordinately suppresses the levels of β_1 (47) or α_{olf} (39), suggesting a functional association between them. To determine whether loss of γ_3 produces a similar effect, we performed immunoblot analysis to compare the levels of various α and β subunits in several brain regions from *Gng3*$^{+/+}$ and *Gng3*$^{-/-}$ mice. The type and extent of suppression was found to differ between brain regions (Fig. 7). In this regard, the level of β_1 was reduced by 24% ± 11% in the cerebellum, while levels of β_2 were reduced by 11% ± 2%, 28% ± 16%, and 42% ± 27% in the striatum, cortex, and cerebellum, respectively (Fig. 7B). No significant decreases in the levels of α_{i1}, α_{i2}, $\alpha_{q/11}$, α_o, α_s, α_{olf}, α_{12}, or α_{13} were observed in the cerebellums, cortices, hippocampi, or striata of *Gng3*$^{-/-}$ mice (data not shown). However, small decreases of 13% ± 8% to 28% ± 16% in the levels of α_{i3} were seen in cortices, hippocampi, and cerebellums of *Gng3*$^{-/-}$ mice, with two different antisera cross-reacting with α_{i1} and α_{i3} showing a decrease, but an antiserum specific for α_{i1} showing no difference (Fig. 7D).

To provide physiological meaning for the observed changes, we next performed quantitative immunoblot analysis on several brain regions from wild-type mice (Fig. 8). The level of β_2 was found to be approximately equal to that of γ_3 in the cortices and cerebellums of wild-type mice (Fig. 8B). Thus, the 30 and 40% reductions in the levels of β_2 in the cortices and cerebellums of *Gng3*$^{-/-}$ mice suggest that γ_3 forms dimers with more than one β subunit in these brain regions of wild-type mice and that loss of γ_3 is accompanied by loss of a $\beta_2\gamma_3$ dimer in these brain regions of *Gng3*$^{-/-}$ mice. The interpretation of the relative reductions in α_{i3} levels in several brain regions is complicated by the lack of specific antisera. Two antisera, which cross-react with α_{i3} and α_{i1} to various degrees, gave different expression levels for α_{i3} in the cortex (Fig. 8D), suggesting that the level of α_{i3} was either equal to or 3 times that of γ_3. If the high-end estimate is correct, the 30% reduction in α_{i3} levels observed in the cortex could be accounted for by the loss of a unique $\alpha_{i3}\beta\gamma_3$ heterotrimer.

Screening of possible receptor signaling pathways affected in *Gng3*$^{-/-}$ mice. The results presented above predict the existence of a specific G_i heterotrimer composed of $\alpha_{i3}\beta\gamma_3$ subunits, whose assembly is limited in certain brain regions of *Gng3*$^{-/-}$ mice. This raises the possibility that one or more receptor signaling pathways whose actions are dependent on this specific G_i heterotrimer may be disrupted in these animals. To test this possibility, we used a novel technique to compare receptor activation of G proteins in brain sections by in vitro autoradiography of [^{35}S]GTPγS binding. Our preliminary screen focused on the mu opioid, A_1 adenosine, and CB_1 cannabinoid receptors, since there was some evidence in the literature to suggest their coupling to G_i proteins and their involvement in signaling pathways affecting neuronal excitability and/or body weight regulation. The agonists DAMGO, PIA, and WIN 55,212-2 were used to visualize mu opioid-, A_1 adenosine-, and CB_1 cannabinoid receptor-stimulated [^{35}S]GTPγS binding, respectively. Visual comparison of autoradiograms from wild-type and *Gng3*$^{-/-}$ mice did not reveal significant

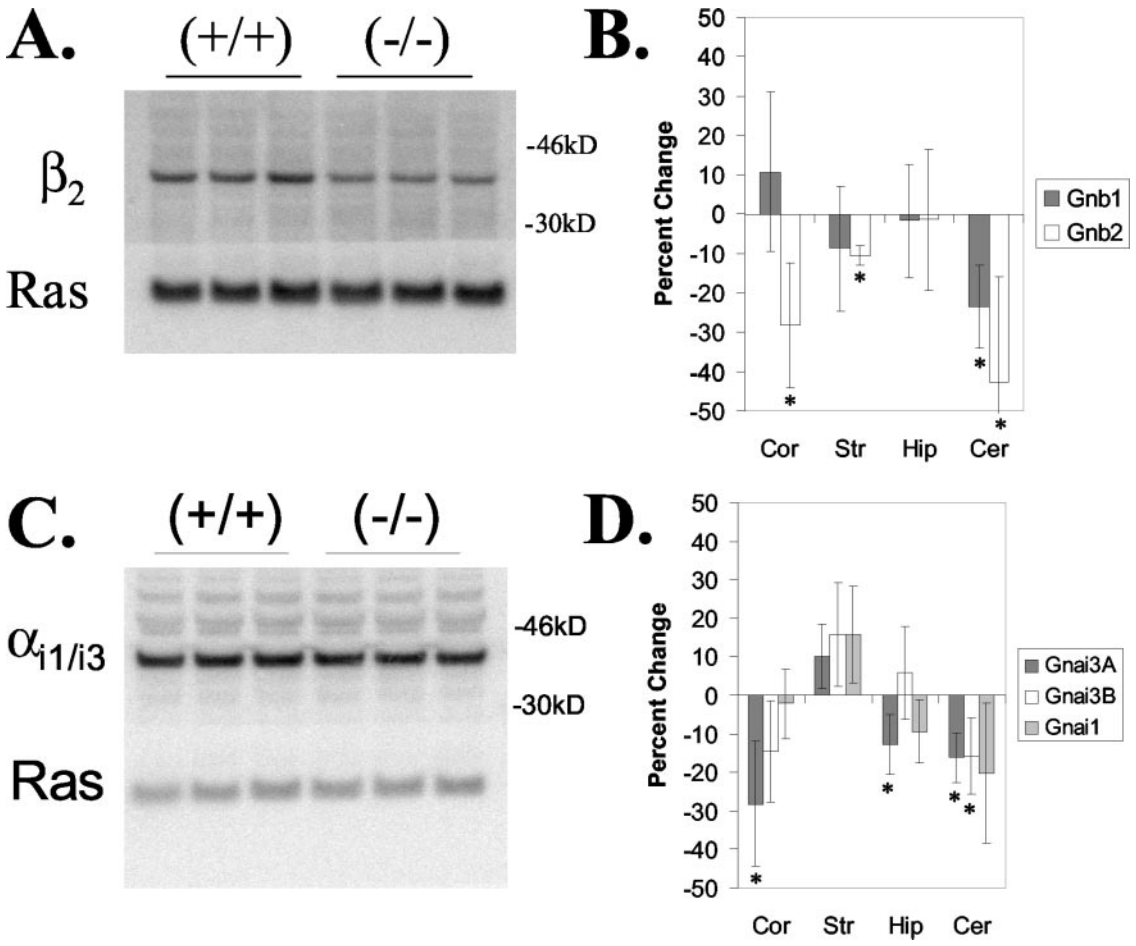

FIG. 7. Expression of α and β subunits in *Gng3*$^{-/-}$ brain regions. (A) Representative immunoblot of β_2 in cerebellum from wild type (+/+) and *Gng3*$^{-/-}$ (−/−) mice; the bottom portion was detected with Ras antisera to control for variations in protein loading. (B) Quantification of immunoblots for β_1 (Gnb1) and β_2 (Gnb2) in the cortex (Cor), striatum (Str), hippocampus (Hip), and cerebellum (Cer). Data are expressed as the percent change from the wild-type level in *Gng3*$^{-/-}$ mice and are means ± standard deviations for three mice in each group. *, $P < 0.05$ for comparison of *Gng3*$^{-/-}$ to *Gng*$^{+/+}$ mice by Student's *t* test. (C) Representative immunoblot of α_{i3} in the cerebellum for wild-type (+/+) and *Gng3*$^{-/-}$ (−/−) mice. The top portion was detected with our $\alpha_{i1/i3}$ antisera; the bottom portion was detected with Ras antisera to control for variations in protein loading. (D) Quantification of immunoblots for α_{i1} (Gnai1) and α_{i3} in four brain regions. Two different antisera for α_{i3}, our $\alpha_{i1/i3}$ antisera (Gnai3A) and Calbiochem α_{i3} antisera (Gnai3B), both cross-reacted with α_{i1} to varying degrees (data not shown). Note that levels of $\alpha_{i1/i3}$ were reduced in the cortex, hippocampus, and cerebellum, but levels of α_{i1} were unchanged in these regions, suggesting that levels of α_{i3} are reduced in these regions.

differences in basal or agonist-stimulated activity in any region. This observation was confirmed by densitometric analysis. Basal [^{35}S]GTPγS binding did not differ between wild-type and *Gng3*$^{-/-}$ mice in the caudate-putamen (232 ± 9 versus 219 ± 7 nCi/g), anterior cingulate cortex (186 ± 8 versus 176 ± 6 nCi/g), hippocampus (202 ± 25 versus 187 ± 5 nCi/g), or hypothalamus (313 ± 23 versus 315 ± 11 nCi/g). Similarly, DAMGO-, WIN 55,212-2-, and PIA-stimulated [^{35}S]GTPγS binding did not differ between wild-type and knockout mice in any region examined (Table 2). Thus, deletion of γ_3 did not appear to affect mu opioid-, A_1 adenosine-, or CB_1 cannabinoid receptor-mediated signaling, at least in the brain regions examined.

Screening of possible effectors in *Gng3*$^{-/-}$ mice. Given the observed reduction in α_{i3} levels in several brain regions of *Gng3*$^{-/-}$ mice, we tested the possibility that inhibition of adenylyl cyclase by one or more G protein-coupled receptors might be disrupted (Fig. 9). As a preliminary screen, we showed that the endogenous cannabinoid receptor agonist anandamide inhibited basal adenylyl cyclase activity equally well in cerebellar membranes from *Gng3*$^{+/+}$ and *Gng3*$^{-/-}$ mice (Fig. 9A), while the A_1 adenosine receptor agonist cyclopentyladenosine inhibited forskolin-stimulated adenylyl cyclase activity equally well in cerebellar membranes from these two lines of mice (Fig. 9B). Thus, deletion of γ_3 did not appear to affect adenylyl cyclase signaling, at least for the receptors and brain regions examined.

DISCUSSION

Gng3$^{-/-}$ mice exhibit a complex phenotype that includes neurological and metabolic abnormalities. The complexity of this phenotype suggests that γ_3 may function in multiple brain regions and/or signaling pathways. In future studies, the ability

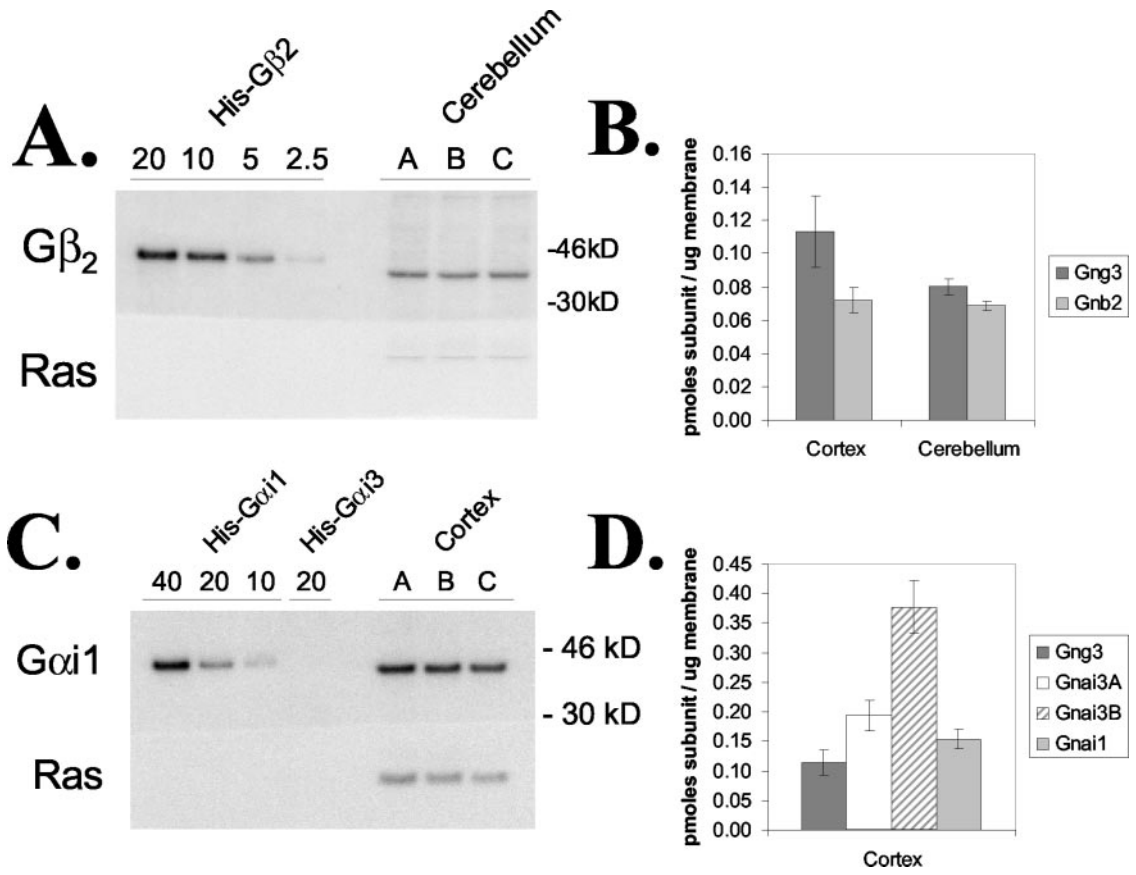

FIG. 8. Quantitative immunoblots of G protein subunits. (A) Representative immunoblot showing a standard curve of the His-tagged β_2 subunit (20, 10, 5, or 2.5 ng/lane) and 20 μg of cholate extracts of cortical membranes from three wild-type mice (mice A, B, and C). The top portion of the blot was incubated with an antiserum for β_2; the bottom portion was incubated with a Ras antiserum to confirm equal loading of the membrane cholate extract. (B) Concentrations of γ_3 and β_2 in the cortex and cerebellum, showing approximately equimolar amounts of both subunits. Data are expressed as picomoles of subunit per microgram of membrane cholate extract and are means ± standard deviations for three mice in each group. (C) Representative immunoblot showing a standard curve of the His-tagged α_{i1} subunit (40, 20, and 10 ng/lane); the His-tagged α_{i3} subunit (20 ng/lane), showing no cross-reactivity with α_{i1} antisera; and 20 μg of cholate extracts of cortical membranes from three wild-type mice (mice A, B, and C). The top portion of the blot was incubated with an antiserum for α_{i1}, and the bottom portion was incubated with a Ras antiserum. (D) Concentrations of γ_3, α_{i1}, and α_{i3} in the cortex. Note that both available α_{i3} antisera cross-reacted with α_{i1} (data not shown) and that the two antisera gave different results, indicating that the concentration of α_{i3} was either equal to or 3 times that of γ_3.

to limit inactivation of the *Gng3* gene to specific brain regions will allow further dissection of the functions of this gene in different neuronal populations.

Seizure-related phenotype. Mice lacking *Gng3* on a mixed genetic background (i.e., FVB/N, C57BL/6, and 129 strains) experience an increased frequency of spontaneous seizures and increased mortality rates compared to their wild-type littermate controls. An association with increased rates of death has been described for other knockout mice with spontaneous seizures. For instance, mice with a deficiency of a serotonin receptor, *Htr2c*, demonstrate spontaneous seizures that occasionally progress to respiratory arrest and death, with

TABLE 2. Densitometric analysis of agonist-stimulated [^{35}S]GTPγS autoradiography in brain regions[a]

Region	[^{35}S]GTPγS binding (mean nCi/g ± SEM)[b] stimulated by the following agonist in the indicated mice[c]:					
	WIN 55,212-2		DAMGO		PIA	
	WT	KO	WT	KO	WT	KO
Cingulate cortex	447 ± 7	438 ± 14	152 ± 24	116 ± 13	495 ± 33	508 ± 16
Caudate-putamen	414 ± 12	405 ± 12	266 ± 26	254 ± 14	363 ± 33	381 ± 8
Hippocampus	413 ± 24	433 ± 18	ND	ND	522 ± 20	506 ± 19
Hypothalamus	242 ± 20	232 ± 9	193 ± 15	196 ± 6	ND	ND

[a] Brain sections were incubated with [^{35}S]GTPγS, GDP, and maximally effective concentrations of the indicated agonists as described in Materials and Methods.
[b] ND, not determined.
[c] WT, wild type; KO, knockout.

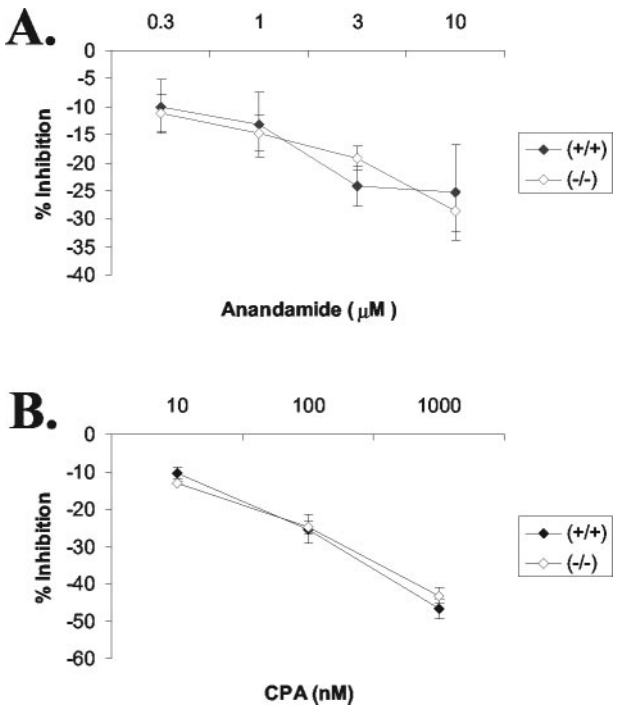

FIG. 9. Adenylyl cyclase assays. (A) Inhibition of adenylyl cyclase by a cannabinoid agonist, 0.3 to 10 μM anandamide, in cerebellar membranes, expressed as percent inhibition of GTP (50 μM)-stimulated activity (119 ± 12 pmol/mg of protein/min for $Gng3^{+/+}$ mice or 125 ± 16 pmol/mg of protein/min for $Gng3^{-/-}$ mice). Data are means ± standard errors for six mice in each group. (B) Inhibition adenylyl cyclase by an A_1 adenosine agonist, 10 to 1,000 nM cyclopentyladenosine (CPA), in cerebellar membranes, expressed as percent inhibition of forskolin (0.3 μM)-stimulated activity (136 ± 20 pmol/mg of protein/min for $Gng3^{+/+}$ mice or 141 ± 13 pmol/mg of protein/min for $Gng3^{-/-}$ mice). Data are means ± standard errors for three mice in each group.

approximately 25% of mice dying by the age of 13 weeks and 50% of mice dying during 25 weeks of observation (46). Mice with a deficiency of the $GABA_{B1}$ receptor, *Gabbr1*, exhibited recurrent spontaneous seizures typified by wild running and limb tonus and clonus, which frequently progressed to death, with a mean life expectancy of only 21 days (36).

Intriguingly, both the spontaneous seizure and mortality phenotypes of $Gng3^{-/-}$ mice are dependent on the genetic background. After crossing onto the C57BL/6J background for 5 generations, these seizure- and mortality-related changes are no longer observed. A similar decline in spontaneous seizures and sudden death was observed when serotonin 5-HT_{2C} receptor-null mice were backcrossed to C57BL/6 mice (18). Notably, these results are consistent with a recent study showing that seizure susceptibility is strain dependent, with the C57BL/6 strain exhibiting a higher electroconvulsive threshold than the FVB/NJ and 129S3 strains (14). To confirm the presence of a modifying factor in the C57BL/6 genome that attenuates the seizure phenotype of $Gng3^{-/-}$ mice, we are currently in the process of backcrossing the $Gng3^{-/-}$ mice to more seizure-sensitive strains.

Although they no longer suffer spontaneous seizures, mice lacking *Gng3* on the C57BL/6J genetic background still exhibit increased seizure susceptibility. A number of mouse models involving disruption of G protein-coupled receptors, their agonists, or intracellular effectors display increased susceptibility to seizures (31). Mice with a deficiency of somatostatin (4), the D2 dopamine receptor (3), or the neuropeptide Y5 receptor (28) all display increased susceptibility to kainic acid-induced seizures. The *Frings* mouse displays audiogenic seizures (44). Mice with a deficiency of neuropeptide Y (11), a serotonin receptor (46), the $GABA_{B1}$ receptor (36), or the GIRK2 potassium channel (42) all exhibit spontaneous or handling-induced seizures. These mouse models suggest potential signaling pathways through which disruption of *Gng3* might increase seizure susceptibility.

Weight-related phenotype. Female mice lacking *Gng3* show reduced body weights, decreased adiposity, and low leptin levels compared to their wild-type littermate controls. Importantly, the phenotype was not dependent on genetic background. The basis for this lean phenotype is currently under investigation. One possibility that was discounted was derangement of *Bscl2* expression as a result of targeting of the *Gng3* gene. The human *BSCL2* gene has been linked to a form of congenital lipodystrophy (27). However, analysis of $Gng3^{-/-}$ mice revealed no disruption of *Bscl2* expression in the brain, white fat, or brown fat. Therefore, the lean phenotype was due to loss of *Gng3* expression. Possibilities under consideration include a change in food consumption and/or metabolic rate. A number of mouse models involving disruption of G protein-coupled receptors or their agonists affect body weight and adiposity. Deficiency of the melanin-concentrating hormone (MCH) prohormone, *Pmch* (41), or its receptor, *Mch1r* (29), produces a lean phenotype in mice as a result of increased metabolic rate. *Mch1r* is coupled to inhibition of adenylyl cyclase (35) and stimulation of calcium channels (16). Deficiency of *Npy2r*, *Npy4r*, or a combination of both receptors produces a lean mouse (38). *Npy2r* is coupled to inhibition of adenylyl cyclase and inhibition of calcium channels through a pertussin toxin-sensitive G protein (40), most likely α_{i3} and unknown $\beta\gamma$ subunits (15). Particular interest revolves around these signaling pathways, since neuropeptide Y affects seizure susceptibility (11). Deficiency of the CB_1 cannabinoid receptor, *Cnr1*, produces mice with a lean phenotype due in part to decreased caloric intake (8). *Cnr1* is coupled to inhibition of presynaptic calcium channels that regulate neurotransmitter release (45). Again, special interest is focused on this signaling pathway, since $Cnr1^{-/-}$ mice showed a mortality phenotype similar to that of our $Gng3^{-/-}$ mice, with ~25% of the mice dying by the age of 6 months (48).

Lack of functional compensation by other γ subtypes. The presence of a phenotype in the $Gng3^{-/-}$ mice suggests that at least some of the functions of γ_3 are unique and cannot be replaced by other related family members. The inability of other subunits to substitute for γ_3 in the context of the organism could be due to a distinctive structural feature or a unique expression pattern of this gene. To begin to distinguish between these possibilities, we examined the effect of loss of γ_3 on other γ subtypes. We showed that loss of γ_3 results in a specific increase in the level of γ_2 in the cortex and the level of γ_7 in the striatum. These results suggest that modest adaptations in γ subunit expression may occur in a region-specific fashion in $Gng3^{-/-}$ mice. Such adaptations may reflect a com-

pensatory change to replace the lost γ_3 in the same signaling pathway. However, based on the relative levels of these γ subtypes within these brain regions, the relatively small changes in γ_2 and γ_7 would not be sufficient to functionally compensate for the much larger loss of γ_3. Alternatively, such changes may reflect a secondary alteration in another signaling pathway or cell type. For example, in situ hybridization studies indicate that γ_3 and γ_7 are expressed in different neuronal populations within the striatum (2). Assuming that this pattern holds true in *Gng3*$^{-/-}$ mice, it suggests that these two γ subtypes normally function in distinct signaling pathways in different cell types, with the changes observed in *Gng3*$^{-/-}$ mice revealing a novel, functional interaction between the two.

Heterotrimeric associations of γ_3. To gain insight into possible associations of γ_3, we have examined the effect of loss of γ_3 on expression of β_1 and β_2 in different regions of the brain. Notably, there were significant reductions in the levels of β_2 in the cortex, striatum, and cerebellum and in the level of β_1 in the cerebellum. In vitro studies have previously demonstrated that the γ subunit enhances the stability of the β subunit; treatment of HEK293 cells with a ribozyme directed against the γ_7 subunit results in a dramatic reduction in the half-life of the β_1 subunit (47). We also examined the effect of loss of γ_3 on levels of the various α subtypes in different regions of the brain. Intriguingly, we found a small, but specific, reduction in the levels of α_{i3} in the cortex, hippocampus, and cerebellum. Further studies will be needed to determine if γ_3 associates with additional α subtypes in these brain regions.

Signal transduction pathways requiring γ3. We have begun to look for possible receptor signaling pathways that are responsible for the observed phenotype of *Gng3*$^{-/-}$ mice. For this purpose, we employed a novel autoradiographic technique that measures receptor-mediated activation of G proteins in brain slices. Focusing on a small subset of receptors and brain regions that could be responsible for the observed phenotype, we saw no differences in mu opioid-, A_1 adenosine-, and CB_1 cannabinoid receptor-stimulated GTPγS binding in selected brain regions between wild-type and *Gng3*$^{-/-}$ mice. Obviously, we need to examine a much larger number of receptors and brain regions. Moreover, by using maximally effective concentrations of the receptor agonist, we may have missed a modest decrease in the potency (i.e., increase in the 50% effective concentration). Nonetheless, there does not appear to be a widespread disruption of receptor-mediated activation of G proteins in the regions examined to date.

Because immunoblot data revealed a small but significant reduction in the α_{i3} subunit levels, we also compared inhibition of adenylyl cyclase activity by the CB_1 cannabinoid and A_1 adenosine receptors. No differences in adenylyl cyclase activity were observed between wild-type and knockout mice, but other possible effectors remain to be examined.

Contrast to *Gng7*$^{-/-}$ mice. Initial characterization of *Gng3*$^{-/-}$ mice reveals a complex phenotype that includes increased seizure susceptibility, decreased body weight, and reduced fat stores. This phenotype was associated with a modest decrease in the level of α_{i3} and no disruption of adenylyl cyclase signaling in several brain regions of *Gng3*$^{-/-}$ mice. Importantly, the phenotype of *Gng3*$^{-/-}$ mice contrasts sharply with that of *Gng7*$^{-/-}$ mice. *Gng7*$^{-/-}$ mice had no observable seizure activity and had normal body weight. However, they displayed an increased acoustic startle response and a trend toward decreased exploratory locomotor activity. This phenotype was associated with a decreased level of α_{olf} and disruption of D_1 dopamine receptor-stimulated adenylyl cyclase signaling in the striatum (39). Because γ_3 and γ_7 are structurally similar and are predominantly expressed in the brain, the finding that mice lacking one or the other subtype display distinctive phenotypes provides conclusive proof that they perform nonredundant roles in separate signaling pathways or biological processes. Collectively, these results support the notion that the γ subunit composition contributes to the specificity of signaling pathways in the context of the organism.

ACKNOWLEDGMENTS

We are indebted to the outstanding technicians in our animal care facility: Cynthia J. Rhone, Gail L. Gregory, and Shannon Wescott. We are grateful to Sigrid Wattler and Michael C. Nehls at Lexicon Genetics, Inc., for the construction of the *Gng3*$^{+/fl}$ mice. We thank Nicole Schechter for technical assistance with the GTPγS binding.

This work was supported by NIH grants GM39867 (awarded to J.D.R.), DA-10770 and DA-05274 (awarded to D.E.S.), and DA-14277 (awarded to L.J.S.-S.).

REFERENCES

1. **Asano, T., R. Morishita, K. Ohashi, M. Nagahama, T. Miyake, and K. Kato.** 1995. Localization of various forms of the γ subunit of G protein in neural and nonneural tissues. J. Neurochem. **64:**1267–1273.
2. **Betty, M., S. W. Harnish, K. J. Rhodes, and M. I. Cockett.** 1998. Distribution of heterotrimeric G-protein β and γ subunits in the rat brain. Neuroscience **85:**475–486.
3. **Bozzi, Y., D. Vallone, and E. Borrelli.** 2000. Neuroprotective role of dopamine against hippocampal cell death. J. Neurosci. **20:**8643–8649.
4. **Buckmaster, P. S., V. Otero-Corchon, M. Rubinstein, and M. J. Low.** 2002. Heightened seizure severity in somatostatin knockout mice. Epilepsy Res. **48:**43–56.
5. **Cali, J. J., E. A. Balcueva, I. Rybalkin, and J. D. Robishaw.** 1992. Selective tissue distribution of G protein γ subunits, including a new form of the γ subunits identified by cDNA cloning. J. Biol. Chem. **267:**24023–24027.
6. **Childers, S. R., T. Sexton, and M. B. Roy.** 1994. Effects of anandamide on cannabinoid receptors in rat brain membranes. Biochem. Pharmacol. **47:** 711–715.
7. **Clapham, D. E., and E. J. Neer.** 1997. G protein $\beta\gamma$ subunits. Annu. Rev. Pharmacol. Toxicol. **37:**167–203.
8. **Cota, D., G. Marsicano, M. Tschop, Y. Grubler, C. Flachskamm, M. Schubert, D. Auer, A. Yassouridis, C. Thone-Reineke, S. Ortmann, F. Tomassoni, C. Cervino, E. Nisoli, A. C. Linthorst, R. Pasquali, B. Lutz, G. K. Stalla, and U. Pagotto.** 2003. The endogenous cannabinoid system affects energy balance via central orexigenic drive and peripheral lipogenesis. J. Clin. Investig. **112:**423–431.
9. **Degtiar, V. E., B. Wittig, G. Schultz, and F. Kalkbrenner.** 1996. A specific G_o heterotrimer couples somatostatin receptors to voltage-gated calcium channels in RINm5F cells. FEBS Lett. **380:**137–141.
10. **Downes, G. B., N. G. Copeland, N. A. Jenkins, and N. Gautam.** 1998. Structure and mapping of the G protein γ3 subunit gene and a divergently transcribed novel gene, Gng3lg. Genomics **53:**220–230.
11. **Erickson, J. C., K. E. Clegg, and R. D. Palmiter.** 1996. Sensitivity to leptin and susceptibility to seizures of mice lacking neuropeptide Y. Nature **381:** 415–421.
12. **Evanko, D. S., M. M. Thiyagarajan, D. P. Siderovski, and P. B. Wedegaertner.** 2001. G$\beta\gamma$ isoforms selectively rescue plasma membrane localization and palmitoylation of mutant Gα_s and Gα_q. J. Biol. Chem. **276:**23945–23953.
13. **Foster, K. A., P. J. McDermott, and J. D. Robishaw.** 1990. Expression of G proteins in rat cardiac myocytes: effect of KCl depolarization. Am. J. Physiol. **259:**H432–H441.
14. **Frankel, W. N., L. Taylor, B. Beyer, B. L. Tempel, and H. S. White.** 2001. Electroconvulsive thresholds of inbred mouse strains. Genomics **74:**306–312.
15. **Freitag, C., A. B. Svendsen, N. Feldthus, K. Lossl, and S. P. Sheikh.** 1995. Coupling of the human Y2 receptor for neuropeptide Y and peptide YY to guanine nucleotide inhibitory proteins in permeabilized SMS-KAN cells. J. Neurochem. **64:**643–650.
16. **Gao, X.-B., and A. N. van den Pol.** 2002. Melanin-concentrating hormone depresses L-, N-, and P/Q-type voltage-dependent calcium channels in rat lateral hypothalamic neurons. J. Physiol. **542:**273–286.
17. **Gautam, N., J. Northup, H. Tamir, and M. I. Simon.** 1990. G protein diversity is increased by associations with a variety of γ subunits. Proc. Natl. Acad. Sci. USA **87:**7973–7977.

18. **Heisler, L. K., H.-M. Chu, and L. H. Tecott.** 1998. Epilepsy and obesity in serotonin 5-HT_{2C} receptor mutant mice. Ann. N. Y. Acad. Sci. **861:**74–78.
19. **Johnson, R. A., R. Alvarez, and Y. Salomon.** 1994. Determination of adenylyl cyclase catalytic activity using single and double column procedures. Methods Enzymol. **238:**31–56.
20. **Iñiguez-Lluhi, J. A., M. I. Simon, J. D. Robishaw, and A. G. Gilman.** 1992. G protein βγ subunits synthesized in Sf9 cells. J. Biol. Chem. **267:**23409–23417.
21. **Kawai, H., M. L. Allende, R. Wada, M. Kono, K. Sango, C. Deng, T. Miyakawa, J. N. Crawley, N. Werth, U. Bierfreund, K. Sandhoff, and R. L. Proia.** 2001. Mice expressing only monosialoganglioside GM3 exhibit lethal audiogenic seizures. J. Biol. Chem. **276:**6885–6888.
22. **Liang, J. J., M. Cockett, and X. Z. Khawaja.** 1998. Immunohistochemical localization of G protein β1, β2, β3, β4, β5, and γ3 subunits in the adult rat brain. J. Neurochem. **71:**345–355.
23. **Lim, W. K., C. S. Myung, J. C. Garrison, and R. R. Neubig.** 2001. Receptor-G protein γ specificity: γ_{11} shows unique potency for A_1 adenosine and 5-HT_{1A} receptors. Biochemistry **40:**10532–10541.
24. **Lodowski, D. T., J. A. Pitcher, W. D. Capel, R. J. Lefkowitz, and J. J. Tesmer.** 2003. Keeping G proteins at bay: a complex between G protein-coupled receptor kinase 2 and Gβγ. Science **300:**1256–1262.
25. **Macrez-Leprêtre, N., F. Kalkbrenner, G. Schultz, and J. Mironneau.** 1997. Distinct functions of G_q and G_{11} proteins in coupling α_1-adrenoreceptors to Ca^{2+} release and Ca^{2+} entry in rat portal vein myocytes. J. Biol. Chem. **272:**5261–5268.
26. **Macrez-Leprêtre, N., F. Kalkbrenner, J.-L. Morel, G. Schultz, and J. Mironneau.** 1997. G protein heterotrimer $G\alpha_{13}\beta_1\gamma 3$ couples the angiotensin AT_{1A} receptor to increases in cytoplasmic Ca^{2+} in rat portal vein myocytes. J. Biol. Chem. **272:**10095–10102.
27. **Magré, J., M. Delépine, E. Khallouf, T. Gedde-Dahl, Jr., L. Van Maldergem, E. Sobel, J. Papp, M. Meier, A. Mégarbané, A. Bachy, A. Verloes, F. H. d'Abronzo, E. Seemanova, R. Assan, N. Baudic, C. Bourut, P. Czernichow, F. Huet, F. Grigorescu, M. de Kerdanet, D. Lacombe, P. Labrune, M. Lanza, H. Loret, F. Matsuda, J. Navarro, A. Nivelon-Chevalier, M. Polak, J. J. Robert, P. Tric, N. Tubiana-Rufi, C. Vigouroux, J. Weissenbach, S. Savasta, J. A. Maassen, O. Trygstad, P. Bogalho, P. Freitas, J. L. Medina, F. Bonnicci, B. I. Joffe, G. Loyson, V. R. Panz, F. J. Raal, S. O'Rahilly, T. Stephenson, C. R. Kahn, M. Lathrop, and J. Capeau.** 2001. Identification of the gene altered in Berardinelli-Seip congenital lipodystrophy on chromosome 11q13. Nat. Genet. **28:**365–370.
28. **Marsh, D. J., S. C. Baraban, G. Hollopeter, and R. D. Palmiter.** 1999. Role of the Y5 neuropeptide Y receptor in limbic seizures. Proc. Natl. Acad. Sci. USA **96:**13518–13523.
29. **Marsh, D. J., D. T. Weingarth, D. E. Novi, H. Y. Chen, M. E. Trumbauer, A. S. Chen, X. M. Guan, M. M. Jiang, Y. Feng, R. E. Camacho, Z. Shen, E. G. Frazier, H. Yu, J. M. Metzger, S. J. Kuca, L. P. Shearman, S. Gopal-Truter, D. J. MacNeil, A. M. Strack, D. E. MacIntyre, L. H. Van der Ploeg, and S. Qian.** 2002. Melanin-concentrating hormone 1 receptor-deficient mice are lean, hyperactive, and hyperphagic and have altered metabolism. Proc. Natl. Acad. Sci. USA **99:**3240–3245.
30. **Mazzoni, M. R., S. Taddei, L. Giusti, P. Rovero, C. Galoppini, A. D'Ursi, S. Albrizio, A. Triolo, E. Novellino, G. Greco, A. Lucacchini, and H. E. Hamm.** 2000. A $G\alpha_s$ carboxyl-terminal peptide prevents G_s activation by the A_{2A} adenosine receptor. Mol. Pharmacol. **58:**226–236.
31. **Meisler, M. H., J. Kearney, R. Ottman, and A. Escayg.** 2001. Identification of epilepsy genes in human and mouse. Annu. Rev. Genet. **35:**567–588.
32. **Moore, R. J., R. Xiao, L. J. Sim-Selley, and S. R. Childers.** 2000. Agonist-stimulated [^{35}S]GTPγS binding in brain: modulation by endogenous adenosine. Neuropharmacology **39:**282–289.
33. **Morishita, R., S. Saga, N. Kawamura, Y. Hashizume, T. Inagaki, K. Kato, and T. Asano.** 1997. Differential localization of the γ_3 and γ_{12} subunits of G proteins in the mammalian brain. J. Neurochem. **68:**820–827.
34. **Morishita, R., H. Shinohara, H. Ueda, K. Kato, and T. Asano.** 1999. High expression of the γ_5 isoform of G protein in neuroepithelial cells and its replacement of the γ_2 isoform during neuronal differentiation in the rat brain. J. Neurochem. **73:**2369–2374.
35. **Pissios, P., D. J. Trombly, I. Tzameli, and E. Maratos-Flier.** 2003. Melanin-concentrating hormone receptor 1 activates extracellular signal-regulated kinase and synergizes with G_s-coupled pathways. Endocrinology **144:**3514–3523.
36. **Prosser, H. M., C. H. Gill, W. D. Hirst, E. Grau, M. Robbins, A. Calver, E. M. Soffin, C. E. Farmer, C. Lanneau, J. Gray, E. Schenck, B. S. Warmerdam, C. Clapham, C. Reavill, D. C. Rogers, T. Stean, N. Upton, K. Humphreys, A. Randall, M. Geppert, C. H. Davies, and M. N. Pangalos.** 2001. Epileptogenesis and enhanced prepulse inhibition in $GABA_{B1}$-deficient mice. Mol. Cell. Neurosci. **17:**1059–1070.
37. **Robishaw, J. D., and C. H. Berlot.** 2004. Translating G protein subunit diversity into functional specificity. Curr. Opin. Cell Biol. **16:**1–4.
38. **Sainsbury, A., P. A. Baldock, C. Schwarzer, N. Ueno, R. F. Enriquez, M. Couzens, A. Inui, H. Herzog, and E. M. Gardiner.** 2003. Synergistic effects of Y2 and Y4 receptors on adiposity and bone mass revealed in double knockout mice. Mol. Cell. Biol. **23:**5225–5233.
39. **Schwindinger, W. F., K. S. Betz, K. E. Giger, A. Sabol, S. K. Bronson, and J. D. Robishaw.** 2003. Loss of G protein γ_7 alters behavior and reduces striatal α_{olf} level and cAMP production. J. Biol. Chem. **278:**6575–6579.
40. **Shigeri, Y., and M. Fujimoto.** 1994. Y2 receptors for neuropeptide Y are coupled to three intracellular signal transduction pathways in a human neuroblastoma cell line. J. Biol. Chem. **269:**8842–8848.
41. **Shimada, M., N. A. Tritos, B. B. Lowell, J. S. Flier, and E. Maratos-Flier.** 1998. Mice lacking melanin-concentrating hormone are hypophagic and lean. Nature **396:**670–674.
42. **Signorini, S., Y. J. Liao, S. A. Duncan, L. Y. Jan, and M. Stoffel.** 1997. Normal cerebellar development but susceptibility to seizures in mice lacking G protein-coupled, inwardly rectifying K^+ channel GIRK2. Proc. Natl. Acad. Sci. USA **94:**923–927.
43. **Sim, L. J., D. E. Selley, and S. R. Childers.** 1995. In vitro autoradiography of receptor-activated G-proteins in rat brain by agonist-stimulated guanylyl 5′-[γ-[^{35}S]thio]-triphosphate binding. Proc. Natl. Acad. Sci. USA **92:**7242–7246.
44. **Skradski, S. L., A. M. Clark, H. Jiang, H. S. White, Y. H. Fu, and L. J. Ptacek.** 2001. A novel gene causing a Mendelian audiogenic mouse epilepsy. Neuron **31:**537–544.
45. **Sullivan, J. M.** 1999. Mechanisms of cannabinoid-receptor-mediated inhibition of synaptic transmission in cultured hippocampal pyramidal neurons. J. Neurophysiol. **82:**1286–1294.
46. **Tecott, L. H., L. M. Sun, S. F. Akana, A. M. Strack, D. H. Lowenstein, M. F. Dallman, and D. Julius.** 1995. Eating disorder and epilepsy in mice lacking 5-HT_{2c} serotonin receptors. Nature **374:**542–546.
47. **Wang, Q., B. K. Mullah, and J. D. Robishaw.** 1999. Ribozyme approach identifies a functional association between the G protein $\beta_1\gamma_7$ subunits in the β-adrenergic receptor signaling pathway. J. Biol. Chem. **274:**17365–17371.
48. **Zimmer, A., A. M. Zimmer, A. G. Hohmann, M. Herkenham, and T. I. Bonner.** 1999. Increased mortality, hypoactivity, and hypoalgesia in cannabinoid CB1 receptor knockout mice. Proc. Natl. Acad. Sci. USA **96:**5780–5785.